Electronic Supplementary Information

for

In Situ Spectroelectrochemical and Theoretical Study on the Oxidation of a 4*H*-Imidazole-Ruthenium Dye Adsorbed on Nanocrystalline TiO_2 Thin Film Electrodes

Ying Zhang,†[a,b] Stephan Kupfer,†[a] Linda Zedler,[a,b] Julian Schindler,[a,b] Thomas Bocklitz,[a] Julien Guthmuller,[c] Sven Rau[d] and Benjamin Dietzek*[a,b]

[a] Y. Zhang, Dr. S. Kupfer, Dr. L. Zedler, J. Schindler, Dr. T. Bocklitz, Prof. Dr. B. Dietzek
Institute of Physical Chemistry
Friedrich Schiller University Jena
Helmholtzweg 4, 07743 Jena, Germany
Fax: (+) 49-3641-948302
E-mail: benjamin.dietzek@uni-jena.de

[b] Y. Zhang, Dr. L. Zedler, J. Schindler, Prof. Dr. B. Dietzek
Leibniz Institute of Photonic Technology Jena (IPHT)
Albert-Einstein-Straße 9, 07745 Jena, Germany

[c] Dr. J. Guthmuller
Faculty of Applied Physics and Mathematics
Gdansk University of Technology,
Narutowicza 11/12, 80233 Gdansk, Poland

[d] Prof. Dr. S. Rau
Institute of Inorganic Chemistry I
University Ulm
Albert-Einstein-Allee 11, 89081 Ulm, Germany

† Both authors contributed equally to this work.

Table S1: Molecular orbitals involved in the main configurations for the excited states of non-oxidized and oxidized species of **RuIm**.

RuIm		
non-oxidized		
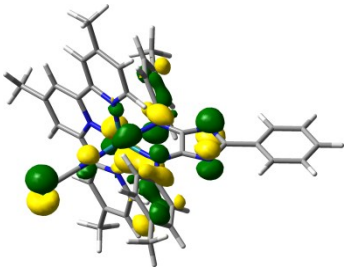	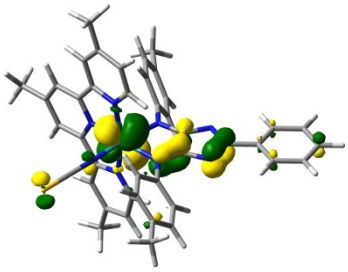	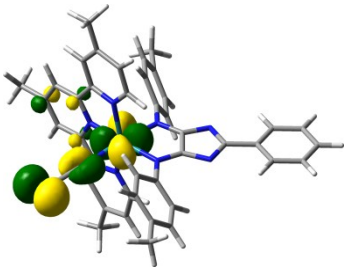
π_{im}(185)	d_{xy}(186)	d_{xz}(187)
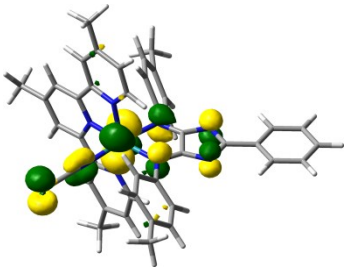	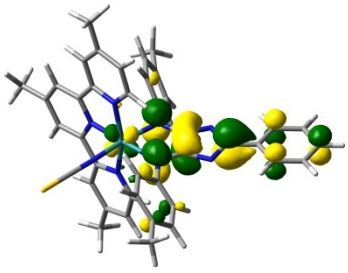	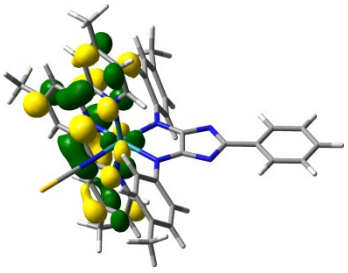
d_{yz}(188)	π^*_{im}(189)	π^*_{tpy}(190)
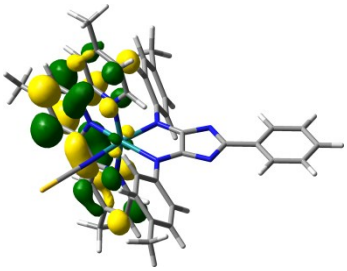		
π^*_{tpy}(191)		
single oxidized		
α-orbitals		
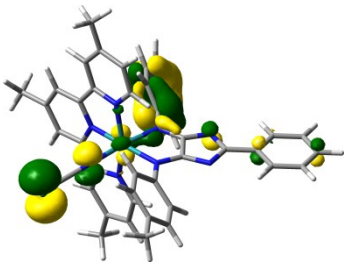	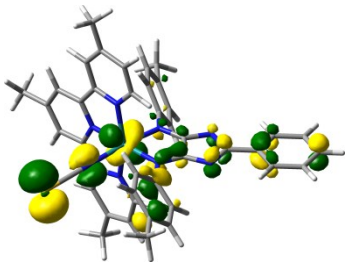	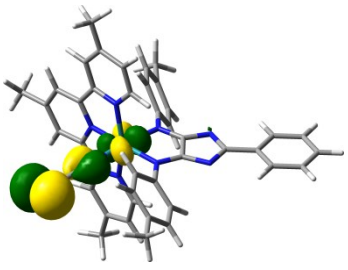
π_{im}(185α)	π_{im}(186α)	$n_{NCS}+d_{xz}$(187α)

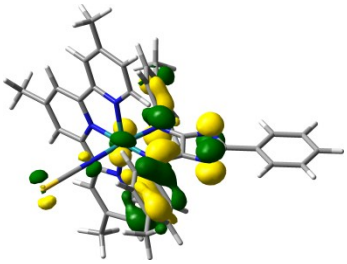

$\pi_{im}(188\alpha)$

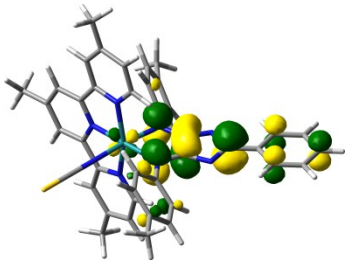

$\pi^*_{im}(189\alpha)$

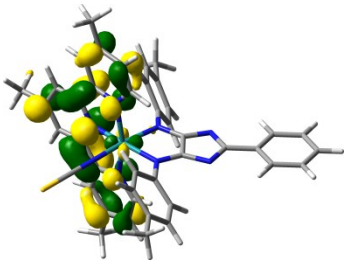

$\pi^*_{tpy}(190\alpha)$

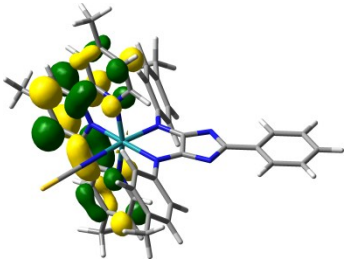

$\pi^*_{tpy}(191\alpha)$

β-orbitals

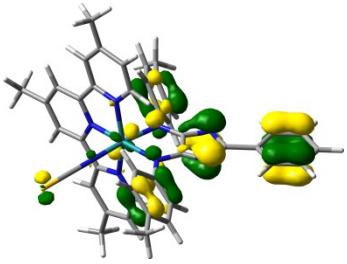

$\pi_{im}(181\beta)$

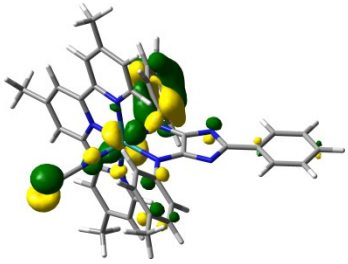

$\pi_{im}(183\beta)$

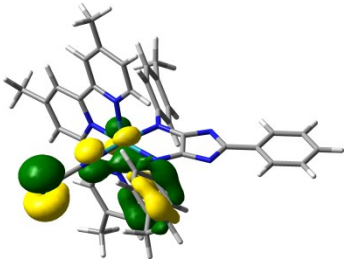

$\pi_{im}(184\beta)$

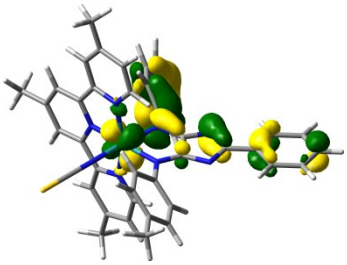

$\pi_{im}(185\beta)$

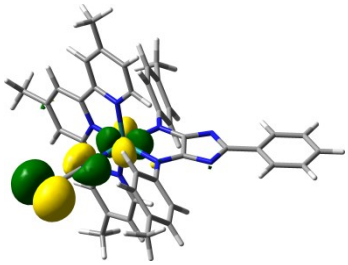

$n_{NCS}+d_{xz}(186\beta)$

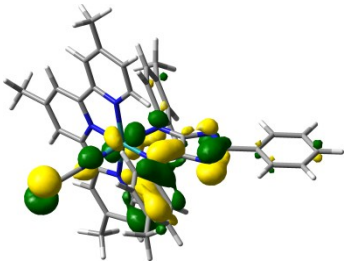

$\pi_{im}(187\beta)$

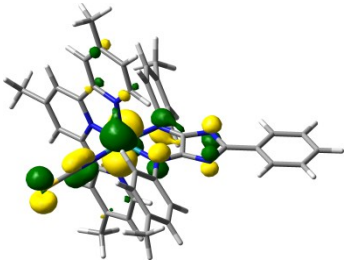

$d_{yz}(188\beta)$

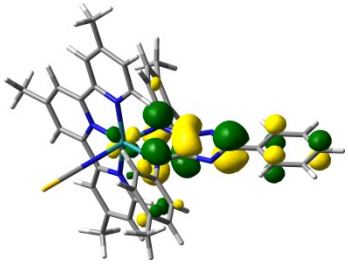

$\pi^*_{im}(189\beta)$

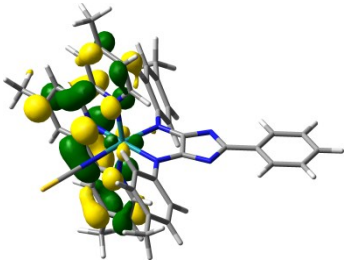

$\pi^*_{tpy}(190\beta)$

Table S2. Calculated bright electronic excited states for the non-oxidized and oxidized species of **RuIm** with the main contributing transitions, excitation energies E^e, oscillator strengths f, the eigen values of ‹s^2›, and experimental absorption maxima.

RuIm							
non-oxidized							
state	transition	weight / %	E^e / eV	λ / nm	f	$\langle s^2 \rangle$	λ_{exp} / nm
S_1	$d_{yz}(188) \rightarrow \pi^*_{im}(189)$ (MLCT)	95	1.87	664	0.037	0.00	700
S_2	$d_{yz}(188) \rightarrow \pi^*_{tpy}(190)$ (MLCT)	95	1.93	644	0.016	0.00	700
S_6	$d_{xz}(187) \rightarrow \pi^*_{tpy}(190)$ (MLCT)	53	2.40	517	0.270	0.00	567
	$d_{xy}(186) \rightarrow \pi^*_{im}(189)$ (MLCT)	36					
S_7	$d_{xz}(187) \rightarrow \pi^*_{tpy}(191)$ (MLCT)	92	2.48	500	0.040	0.00	567
S_8	$d_{xy}(186) \rightarrow \pi^*_{tpy}(191)$ (MLCT)	55	2.52	491	0.072	0.00	567
	$d_{xy}(186) \rightarrow \pi^*_{im}(189)$ (MLCT)	28					
	$d_{xz}(187) \rightarrow \pi^*_{tpy}(190)$ (MLCT)	9					
S_9	d_{xy} 186) $\rightarrow \pi^*_{tpy}(191)$ (MLCT)	37	2.65	467	0.141	0.00	427
	$d_{xy}(186) \rightarrow \pi^*_{im}(189)$ (MLCT)	26					
	$d_{xz}(187) \rightarrow \pi^*_{tpy}(190)$ (MLCT)	21					
S_{10}	$\pi_{im}(185) \rightarrow \pi^*_{im}(189)$ (ILCT)	87	2.91	426	0.221	0.00	427
single oxidized							
state	transition	weight / %	E^e / eV	λ / nm	f	$\langle s^2 \rangle$	λ_{exp} / nm
D_3	$\pi_{im}(187\beta) \rightarrow d_{yz}(188\beta)$ (LMCT)	57	1.20	1030	0.053	0.81	900
	$\pi_{im}(185\beta) \rightarrow d_{yz}(188\beta)$ (LMCT)	27					
D_4	$\pi_{im}(184\beta) \rightarrow d_{yz}(188\beta)$ (LMCT)	35	1.68	738	0.056	0.91	900
	$\pi_{im}(185\beta) \rightarrow d_{yz}(188\beta)$ (LMCT)	28					
	$\pi_{im}(183\beta) \rightarrow d_{yz}(188\beta)$ (LMCT)	16					
D_6	$\pi_{im}(184\beta) \rightarrow d_{yz}(188\beta)$ (LMCT)	41	1.84	673	0.063	1.30	900
	$\pi_{im}(183\beta) \rightarrow d_{yz}(188\beta)$ (LMCT)	19					
	$\pi_{im}(188\alpha) \rightarrow \pi^*_{im}(189\alpha)$ (ILCT)	16					
	$\pi_{im}(187\beta) \rightarrow \pi^*_{im}(189\beta)$ (ILCT)	13					
D_{16}	$\pi_{im}(187\beta) \rightarrow \pi^*_{im}(189\beta)$ (ILCT)	30	2.56	484	0.195	1.18	440
	$\pi_{im}(188\alpha) \rightarrow \pi^*_{im}(189\alpha)$ (ILCT)	29					
	$\pi_{im}(185\beta) \rightarrow \pi^*_{im}(189\beta)$ (IL)	15					
D_{22}	$n_{NCS}+d_{xz}(187\alpha) \rightarrow \pi^*_{tpy}(190\alpha)$ (LLCT)	47	2.84	437	0.155	1.05	440
	$n_{NCS}+d_{xz}(186\beta) \rightarrow \pi^*_{tpy}(190\beta)$ (LLCT)	16					
	$\pi_{im}(186\alpha) \rightarrow \pi^*_{im}(189\alpha)$ (IL)	12					
D_{23}	$\pi_{im}(186\alpha) \rightarrow \pi^*_{im}(189\alpha)$ (IL)	28	2.90	428	0.219	1.18	440
	$\pi_{im}(188\alpha) \rightarrow \pi^*_{tpy}(191\alpha)$ (ILCT)	24					
	$\pi_{im}(185\beta) \rightarrow \pi^*_{im}(189\beta)$ (IL)	12					
D_{31}	$\pi_{im}(185\alpha) \rightarrow \pi^*_{im}(189\alpha)$ (ILCT)	37	3.03	409	0.166	1.71	440
	$\pi_{im}(185\beta) \rightarrow \pi^*_{im}(189\beta)$ (IL)	9					
	$\pi_{im}(184\beta) \rightarrow \pi^*_{im}(189\beta)$ (ILCT)	9					
	$\pi_{im}(181\beta) \rightarrow \pi^*_{im}(189\beta)$ (IL)	8					

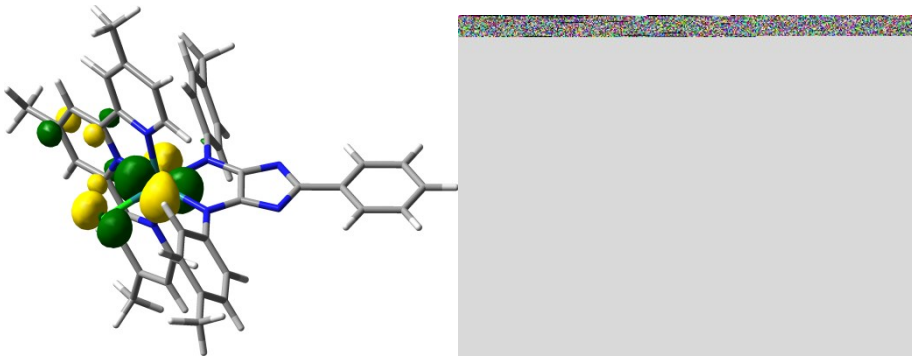

Figure S1. Molecular orbitals $d_{xy}(180)$ of the chloro-4*H*-imidazole-ruthenium complex (left) as compared with molecular orbitals $d_{xy}(187)$ of isothiocyanate **RuIm** (right).

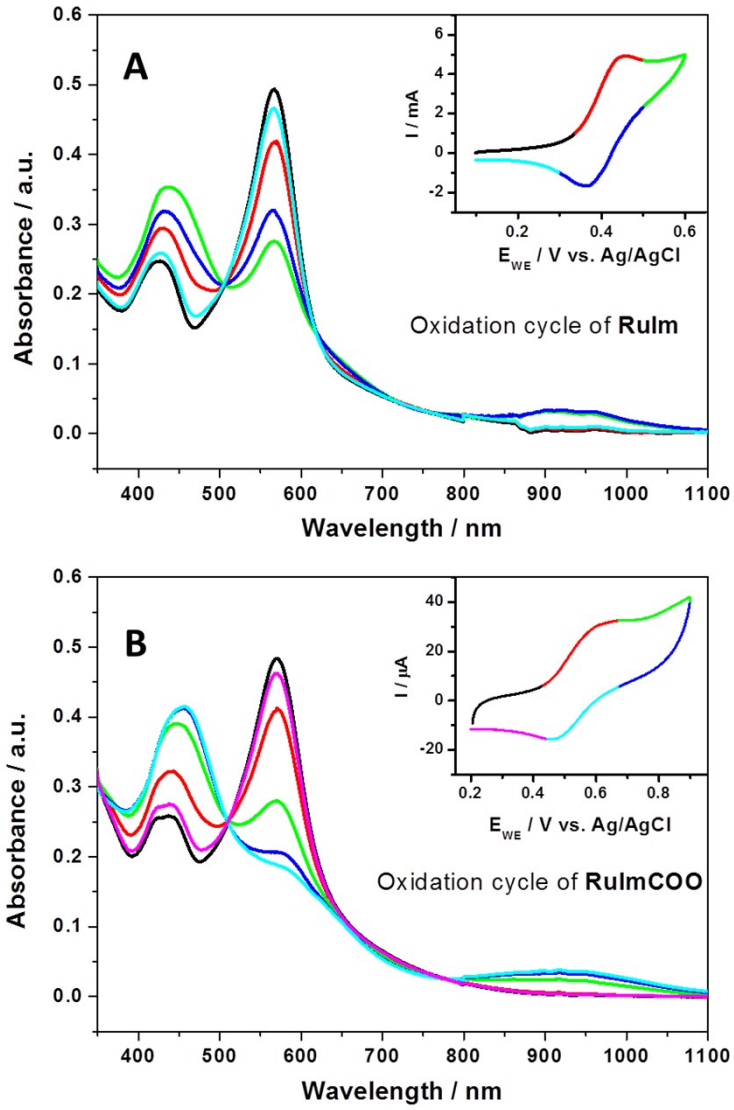

Figure S2. Absorption spectra of **RuIm** (A) and **RuImCOO** (B) in solution during running a CV. The spectra correspond to respective applied potentials of same colors.

Table S3: Total charge density difference between the non-oxidized singlet and the single oxidized doublet ground states within the respective equilibrium geometries of **RuIm**, **RuImCOO** and the respective chloro-complex without anchoring group denoted as **RuCl**.

	Total charge density difference	
	Equilibrium structure	
	Non-oxidized singlet	Single oxidized doublet
RuIm	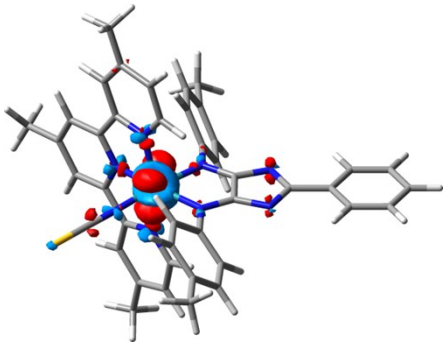	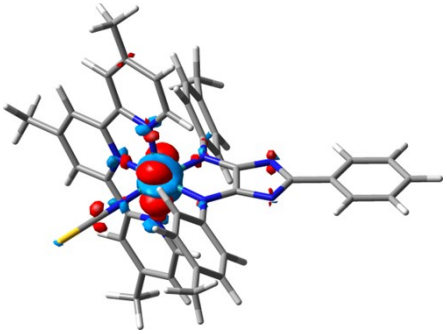
RuImCOO	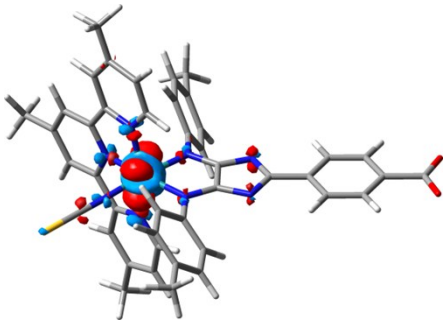	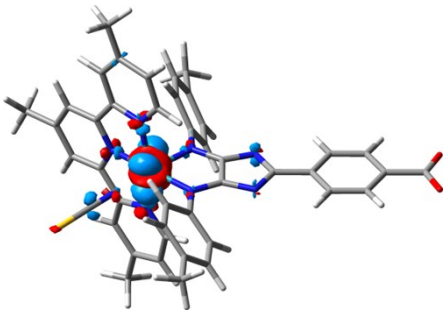
RuCl	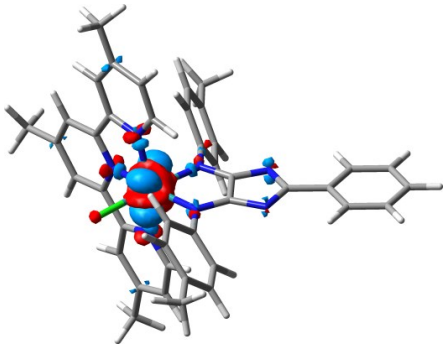	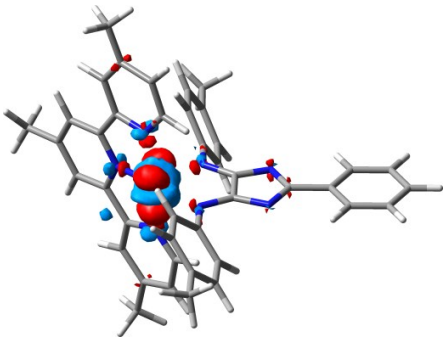

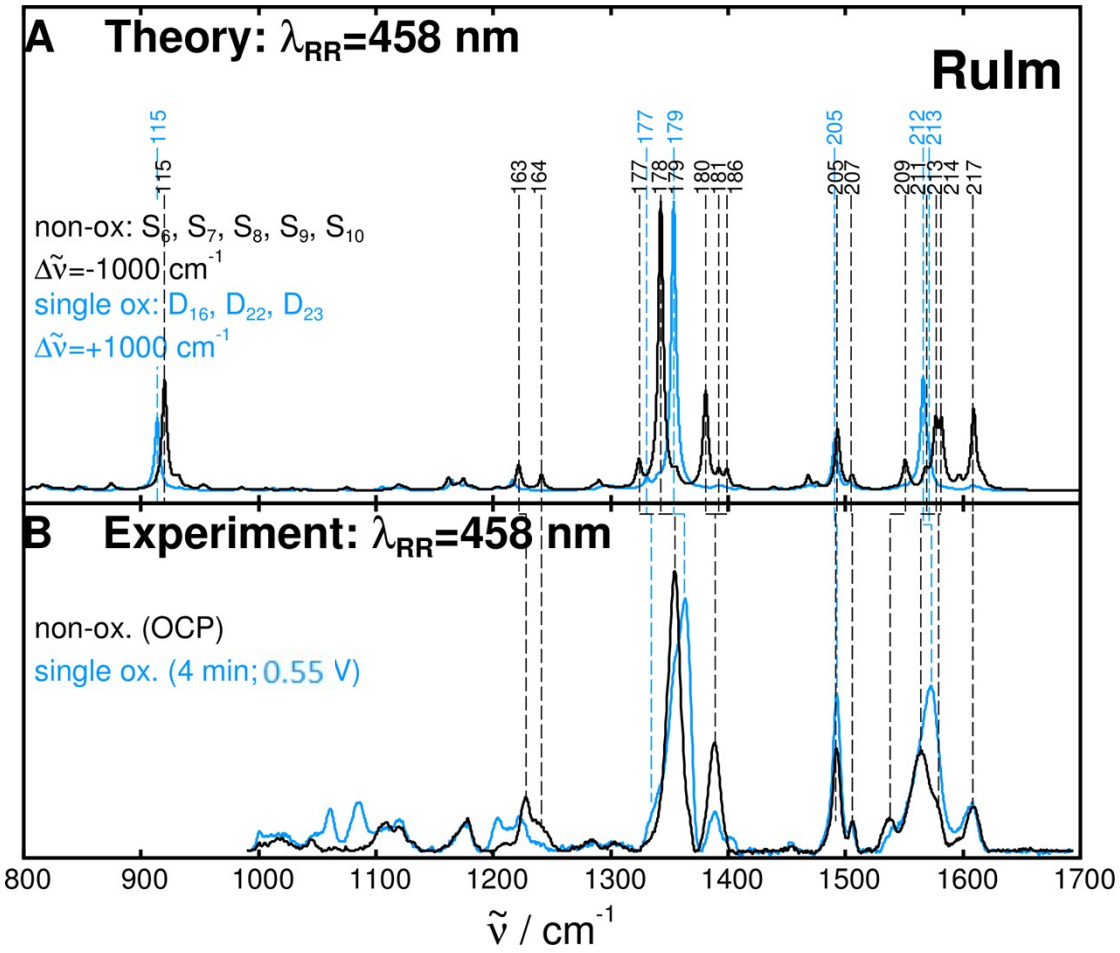

Figure S3. Calculated (A) and experimental (B) RR spectra of non-oxidized (blue) and oxidized (black) species of **RuIm** (λ_{RR} = 458 nm), while the vibrational modes are assigned to the measured bands and labeled accordingly.

Table S4. Vibrational modes of the non-oxidized and oxidized species of **RuIm** with relative RR intensities ≥ 5% (λ_{RR} = 458 nm).

RuIm
non-oxidized
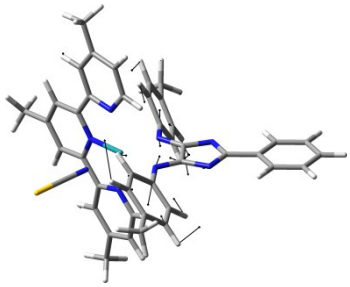 163
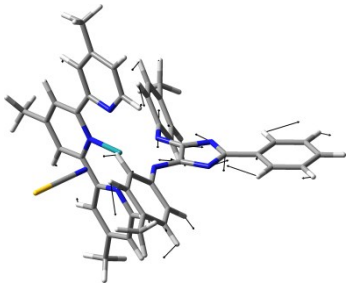 164
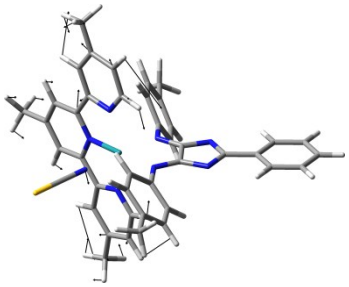 177
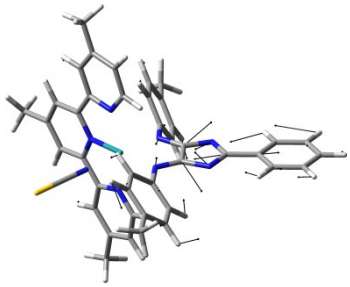 178
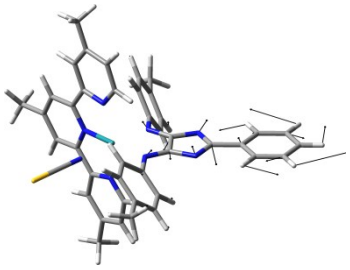 179
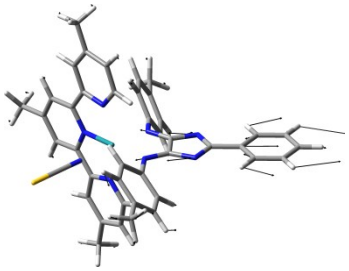 180
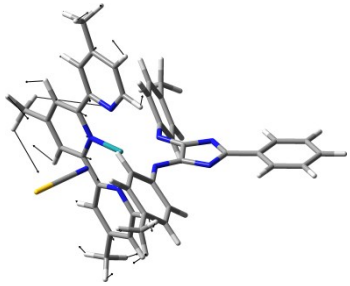 181
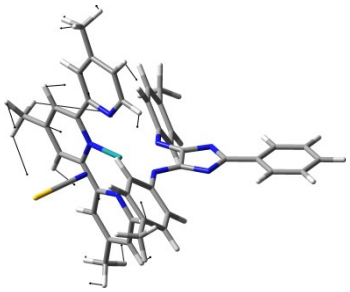 186
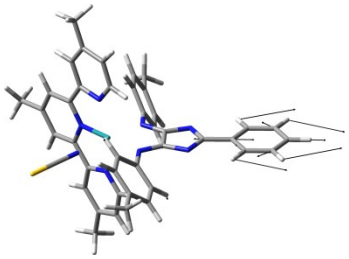 205
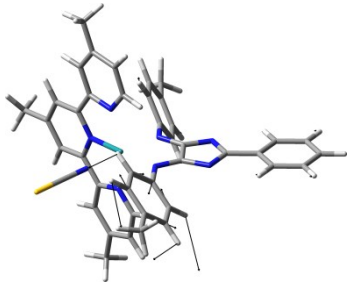 207
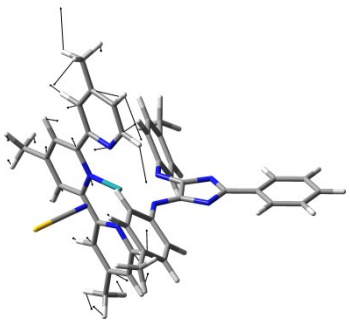 209
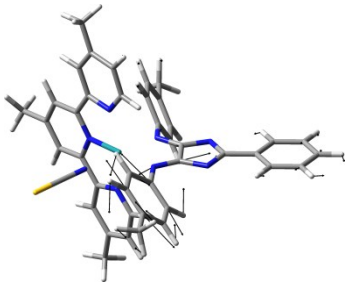 211

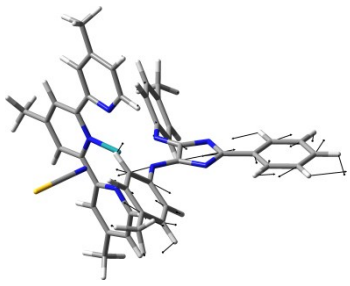	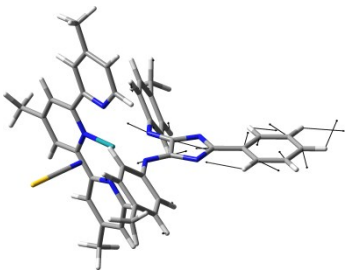	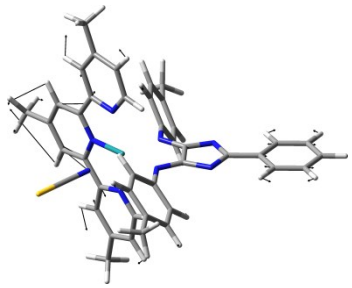
213	214	217
single oxidized		
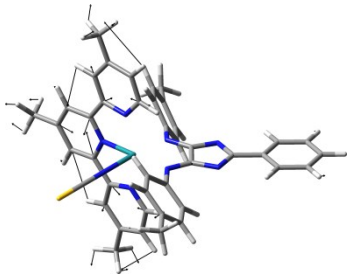	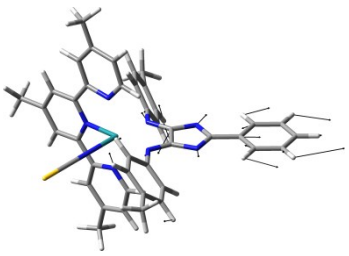	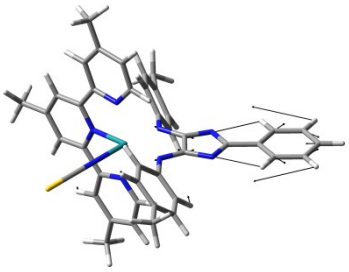
177	179	205
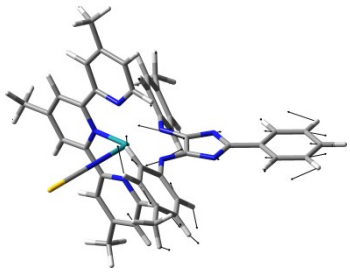	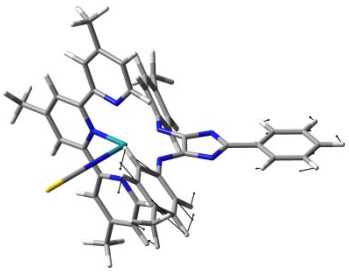	
212	213	

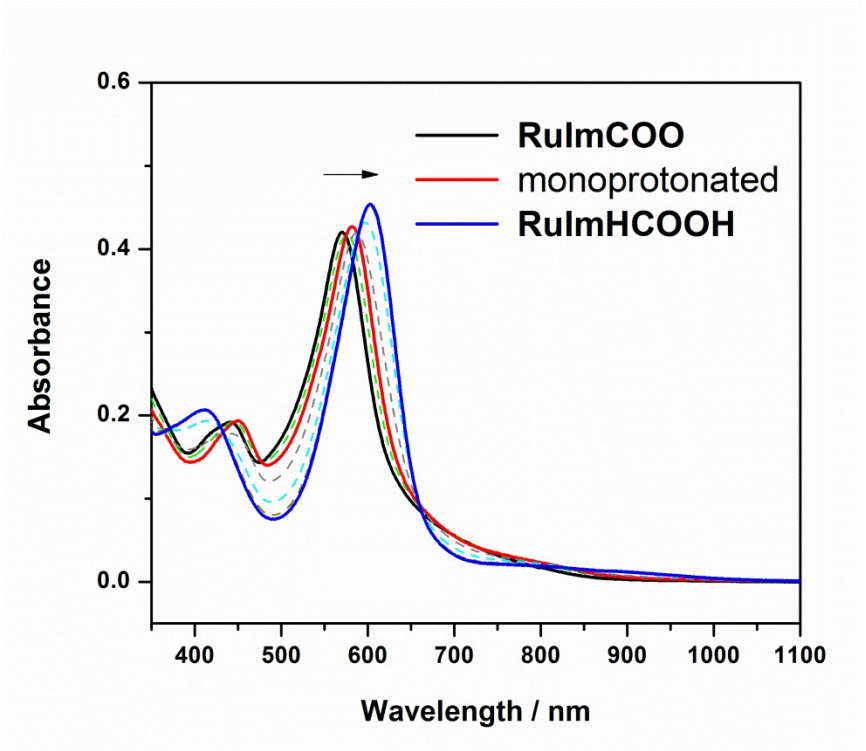

Figure S4. Absorption spectra of the deprotonated **RuImCOO** in ACN on addition of aliquots of TFA acid. The deprotonated form **RuImCOO** is illustrated in black, the single protonated form in red and the double protonated form **RuImHCOOH** in blue.

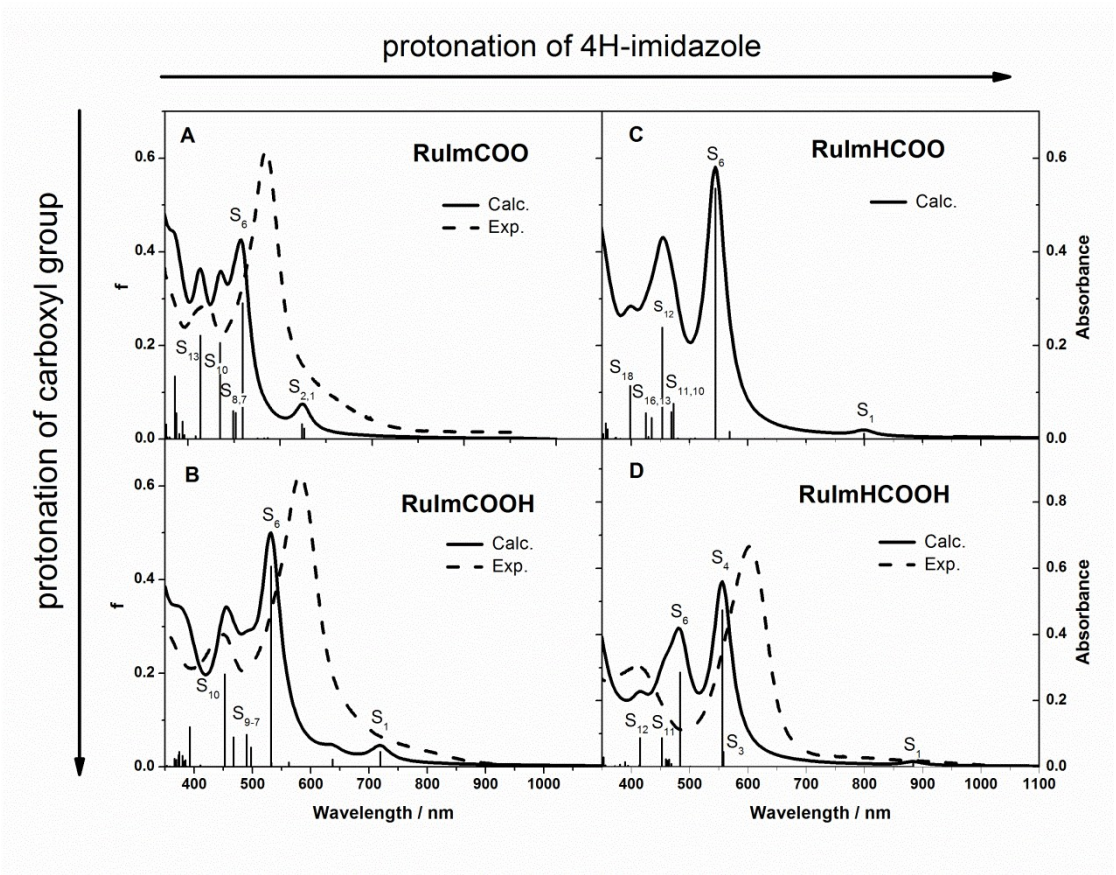

Figure S5. Calculated (solid) and experimental (dashed) absorption spectra for different protonated species of **RuImCOOH** (A-D) in ACN.

Table S5: Molecular orbitals involved in the main configurations for the excited states of non-oxidized and oxidized species of **RuImCOO**.

RuImCOO		
non-oxidized		
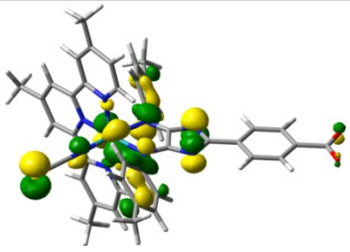	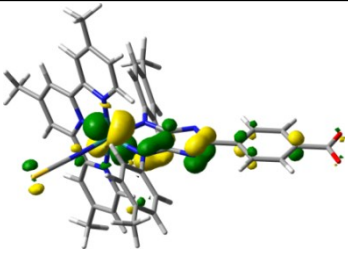	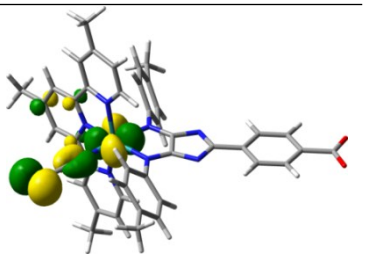
π_{im}(193)	d_{xy}(196)	d_{xz}(198)
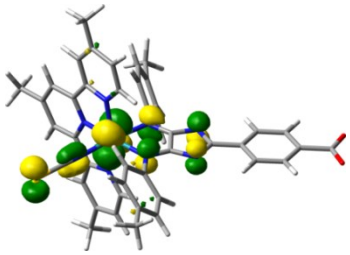	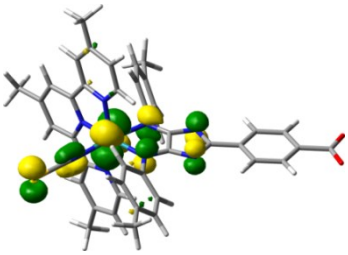	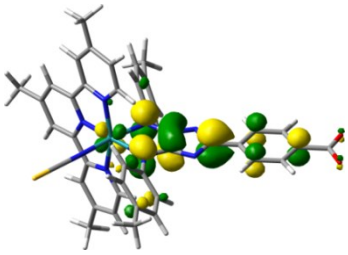
d_{yz}(199)	d_{yz}(199)	π^*_{im}(200)
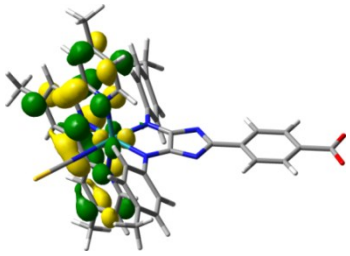	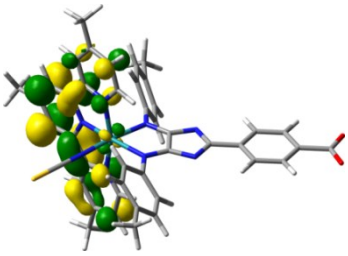	
π^*_{tpy}(201)	π^*_{tpy}(202)	
single oxidized		
α-orbitals		
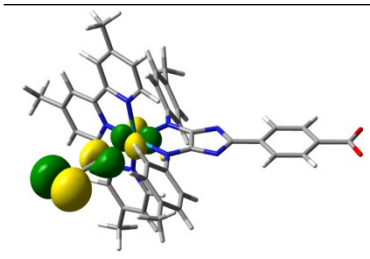	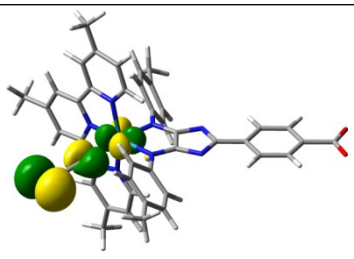	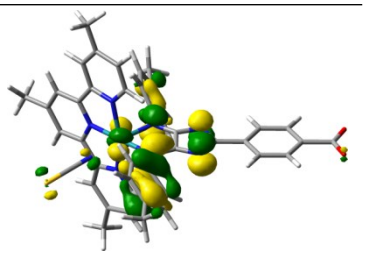
$n_{NCS}+d_{xz}$(194α)	$\pi_{im}+d_{xy}$(195α)	π_{im}(196α)
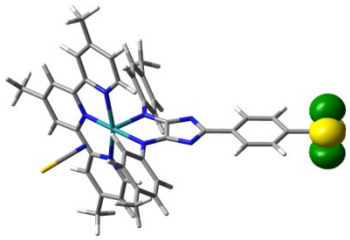	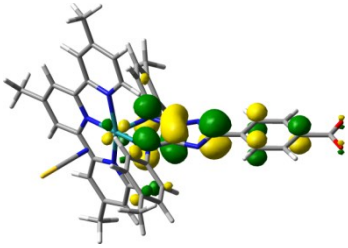	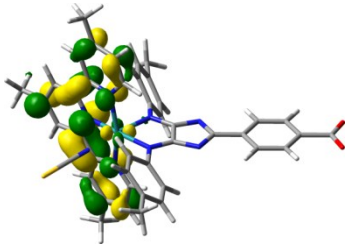
n_{oo}(197α)	π^*_{im}(200α)	π^*_{tpy}(201α)

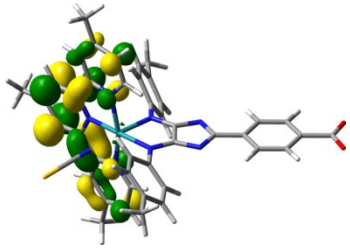

$\pi^*_{tpy}(202\alpha)$

β-orbitals

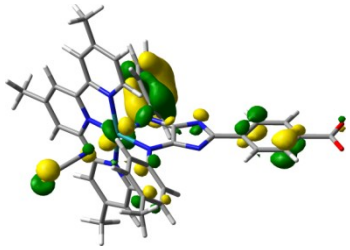

$\pi_{im}(191\beta)$

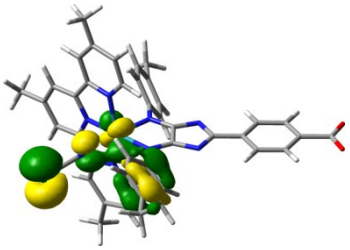

$\pi_{im}(192\beta)$

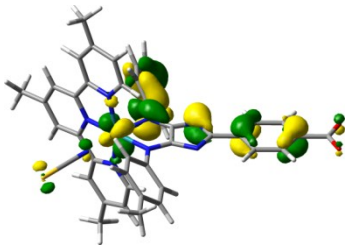

$\pi_{im}(193\beta)$

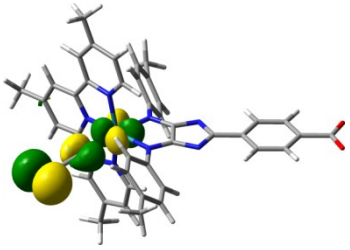

$n_{NCS}+d_{xz}(194\beta)$

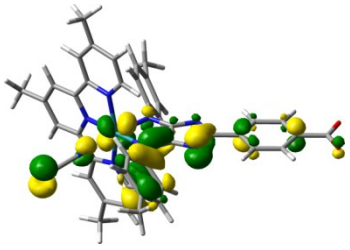

$\pi_{im}(195\beta)$

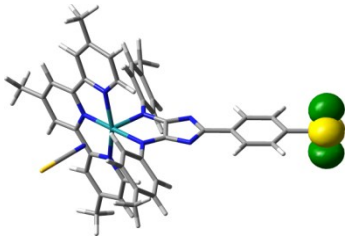

$n_{oo}(196\beta)$

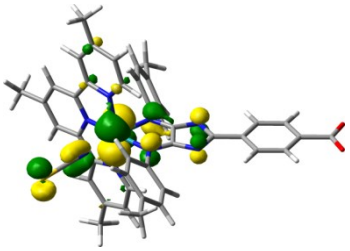

$d_{yz}(199\beta)$

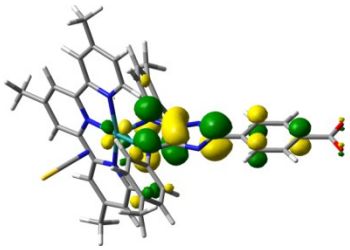

$\pi^*_{im}(200\beta)$

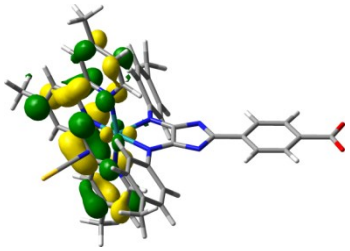

$\pi^*_{tpy}(201\beta)$

Table S6. Calculated bright electronic excited states for the non-oxidized and oxidized species of **RuImCOO** with the main contributing transitions, excitation energies E^e, oscillator strengths f, the eigen values of ‹s^2›, and experimental absorption maxima.

RuImCOO							
non-oxidized							
state	transition	weight / %	E^e / eV	λ / nm	f	$\langle s^2 \rangle$	λ_{exp} / nm
S_1	$d_{yz}(199) \rightarrow \pi^*_{tpy}(201)$ (MLCT)	73	1.90	652	0.023	0.00	700
	$d_{yz}(199) \rightarrow \pi^*_{im}(200)$ (MLCT)	23					
S_2	$d_{yz}(199) \rightarrow \pi^*_{im}(200)$ (MLCT)	74	1.91	648	0.032	0.00	700
	$d_{yz}(199) \rightarrow \pi^*_{tpy}(201)$ (MLCT)	23					
S_6	$d_{xz}(198) \rightarrow \pi^*_{tpy}(201)$ (MLCT)	55	2.39	518	0.291	0.00	570
	$d_{xy}(196) \rightarrow \pi^*_{im}(200)$ (MLCT)	30					
S_7	$d_{xz}(198) \rightarrow \pi^*_{tpy}(202)$ (MLCT)	86	2.46	503	0.056	0.00	570
S_8	$d_{xy}(196) \rightarrow \pi^*_{tpy}(202)$ (MLCT)	63	2.49	498	0.060	0.00	570
	$d_{xy}(196) \rightarrow \pi^*_{im}(200)$ (MLCT)	22					
S_{10}	$d_{xy}196) \rightarrow \pi^*_{im}(200)$ (MLCT)	32	2.64	469	0.206	0.00	420
	$d_{xy}(196) \rightarrow \pi^*_{tpy}(202)$ (MLCT)	27					
	$d_{xz}(198) \rightarrow \pi^*_{tpy}(201)$ (MLCT)	22					
S_{13}	$\pi_{im}(193) \rightarrow \pi^*_{im}(200)$ (ILCT)	87	2.91	426	0.221	0.00	439
single oxidized							
state	transition	weight / %	E^e / eV	λ / nm	f	$\langle s^2 \rangle$	λ_{exp} / nm
D_4	$\pi_{im}(193\beta) \rightarrow d_{yz}(199\beta)$ (LMCT)	42	1.20	1037	0.058	0.81	900
	$\pi_{im}(195\beta) \rightarrow d_{yz}(199\beta)$ (LMCT)	41					
	$\pi_{im}(192\beta) \rightarrow d_{yz}(199\beta)$ (LMCT)	8					
D_7	$\pi_{im}(192\beta) \rightarrow d_{yz}(199\beta)$ (LMCT)	34	1.64	754	0.063	0.89	900
	$\pi_{im}(193\beta) \rightarrow d_{yz}(199\beta)$ (LMCT)	33					
	$\pi_{im}(191\beta) \rightarrow d_{yz}(199\beta)$ (LMCT)	12					
D_9	$\pi_{im}(192\beta) \rightarrow d_{yz}(199\beta)$ (LMCT)	38	1.86	665	0.056	1.37	900
	$\pi_{im}(196\alpha) \rightarrow \pi^*_{im}(200\alpha)$ (ILCT)	18					
	$\pi_{im}(195\beta) \rightarrow \pi^*_{im}(200\beta)$ (ILCT)	13					
	$\pi_{im}(191\beta) \rightarrow d_{yz}(199\beta)$ (LMCT)	13					
D_{25}	$n_{oo}(196\beta) \rightarrow \pi^*_{im}(200\beta)$ (ILCT)	36	2.55	485	0.137	1.01	459
	$\pi_{im}(195\beta) \rightarrow \pi^*_{im}(200\beta)$ (ILCT)	17					
	$n_{oo}(197\alpha) \rightarrow \pi^*_{im}(200\alpha)$ (ILCT)	15					
	$\pi_{im}(196\alpha) \rightarrow \pi^*_{im}(200\alpha)$ (ILCT)	13					
	$\pi_{im}(193\beta) \rightarrow \pi^*_{im}(200\beta)$ (ILCT)	12					
D_{27}	$n_{oo}(196\beta) \rightarrow \pi^*_{im}(200\beta)$ (ILCT)	18	2.58	481	0.085	1.48	459
	$n_{NCS}+d_{xz}(194\beta) \rightarrow \pi^*_{im}(200\beta)$ (ILCT)	18					
	$\pi_{im}(196\alpha) \rightarrow \pi^*_{im}(200\alpha)$ (ILCT)	13					
	$\pi_{im}(195\beta) \rightarrow \pi^*_{im}(200\beta)$ (ILCT)	12					
	$n_{NCS}+d_{xz}(194\beta) \rightarrow \pi^*_{tpy}(201\beta)$ (LLCT)	12					

D_{37}	$n_{NCS}+d_{xz}(194\alpha) \rightarrow \pi^*_{tpy}(201\alpha)$ (LLCT)	29	2.81	441	0.327	1.07	459
	$\pi_{im}+d_{xy}(195\alpha) \rightarrow \pi^*_{im}(200\alpha)$ (ILCT)	18					
	$\pi_{im}(193\beta) \rightarrow \pi^*_{im}(200\beta)$ (ILCT)	13					
	$n_{NCS}+d_{xz}(194\beta) \rightarrow \pi^*_{tpy}(201\beta)$ (LLCT)	12					
	$\pi_{im}+d_{xy}(195\alpha) \rightarrow \pi^*_{tpy}(201\alpha)$ (LLCT)	11					
D_{38}	$\pi_{im}+d_{xy}(195\alpha) \rightarrow \pi^*_{tpy}(201\alpha)$ (LLCT)	57	2.85	435	0.176	1.46	459
	$\pi_{im}+d_{xy}(195\alpha) \rightarrow \pi^*_{im}(200\alpha)$ (ILCT)	13					
D_{39}	$\pi_{im}(196\alpha) \rightarrow \pi^*_{tpy}(202\alpha)$ (ILCT)	45	2.87	432	0.098	1.18	459

Table S7. Calculated bright electronic excited states for the monoprotonated species **RuImCOOH** and **RuImHCOO** with the main contributing transitions, excitation energies E^e, oscillator strengths f, the eigen values of ‹s^2›, and experimental absorption maxima.

RuImCOOH							
state	transition	non-oxidized weight / %	E^e / eV	λ / nm	f	$\langle s^2 \rangle$	λ_{exp} / nm
S_1	$d_{yz}(199) \rightarrow \pi^*_{im}(200)$ (MLCT)	96	1.72	719	0.032	0.00	700
S_6	$d_{xy}(197) \rightarrow \pi^*_{im}(200)$ (MLCT)	64	2.33	532	0.428	0.00	582
	$d_{xz}(198) \rightarrow \pi^*_{tpy}(201)$ (MLCT)	28					
S_7	$d_{xz}(198) \rightarrow \pi^*_{tpy}(202)$ (MLCT)	80	2.49	497	0.041	0.00	582
	$d_{xz}(198) \rightarrow \pi^*_{tpy}(201)$ (MLCT)	9					
S_8	$d_{xz}(198) \rightarrow \pi^*_{tpy}(201)$ (MLCT)	31	2.53	490	0.069	0.00	582
	$d_{xy}(197) \rightarrow \pi^*_{tpy}(202)$ (MLCT)	27					
	$d_{xy}(197) \rightarrow \pi^*_{im}(200)$ (MLCT)	17					
	$d_{xz}(198) \rightarrow \pi^*_{tpy}(202)$ (MLCT)	16					
S_9	$d_{xy}(197) \rightarrow \pi^*_{tpy}(202)$ (MLCT)	65	2.65	468	0.063	0.00	425
	$d_{xz}(198) \rightarrow \pi^*_{tpy}(201)$ (MLCT)	14					
S_{10}	$d_{yz}+\pi_{im}(196) \rightarrow \pi^*_{im}(200)$ (MLCT/ILCT)	90	2.74	452	0.198	0.00	451

RuImHCOO							
state	transition	non-oxidized weight / %	E^e / eV	λ / nm	f	$\langle s^2 \rangle$	λ_{exp} / nm
S_1	$d_{yz}(199) \rightarrow \pi^*_{im}(200)$ (MLCT)	94	1.55	799	0.012	0.00	-
S_6	$d_{xy}(195) \rightarrow \pi^*_{im}(200)$ (MLCT)	81	2.28	544	0.536	0.00	-
	$d_{xz}(197) \rightarrow \pi^*_{tpy}(201)$ (MLCT)	10					
S_{10}	$d_{xz}(197) \rightarrow \pi^*_{tpy}(202)$ (MLCT)	35	2.62	473	0.076	0.00	-
	$d_{xz}(197) \rightarrow \pi^*_{tpy}(201)$ (MLCT)	30					
	$d_{yz}(199) \rightarrow \pi^*_{tpy}(202)$ (MLCT)	19					
S_{11}	$d_{xz}(197) \rightarrow \pi^*_{tpy}(202)$ (MLCT)	62	2.64	469	0.058	0.00	-
	$d_{xz}(197) \rightarrow \pi^*_{tpy}(201)$ (MLCT)	17					
	$d_{yz}(199) \rightarrow \pi^*_{tpy}(202)$ (MLCT)	11					
S_{12}	$\pi_{im}(193) \rightarrow \pi^*_{im}(200)$ (ILCT)	86	2.74	453	0.268	0.00	-
S_{13}	$n_{NCS}+d_{yz}(192) \rightarrow \pi^*_{im}(200)$ (LLCT)	81	2.85	435	0.045	0.00	-
S_{16}	$n_{NCS}+d_{xz}(191) \rightarrow \pi^*_{im}(200)$ (LLCT)	77	2.92	425	0.055	0.00	-
	$d_{xy}(195) \rightarrow \pi^*_{tpy}(202)$ (MLCT)	11					
S_{18}	$\pi_{im}(190) \rightarrow \pi^*_{im}(200)$ (ILCT)	98	3.12	398	0.114	0.00	-

Table S8. Calculated bright electronic excited states for the double-protonated species **RuImHCOOH** with the main contributing transitions, excitation energies E^e, oscillator strengths f, the eigen values of ‹s^2›, and experimental absorption maxima.

RuImHCOOH							
non-oxidized							
state	transition	weight / %	E^e / eV	λ / nm	f	$\langle s^2 \rangle$	λ_{exp} / nm
S_1	$d_{yz}(199) \rightarrow \pi^*_{im}(200)$ (MLCT)	93	1.40	884	0.011	0.00	-
S_3	$d_{yz}(199) \rightarrow \pi^*_{tpy}(201)$ (MLCT)	92	2.22	558	0.045	0.00	603
S_4	$d_{xy}(197) \rightarrow \pi^*_{im}(200)$ (MLCT)	79	2.23	556	0.473	0.00	603
S_6	$\pi_{im}(196) \rightarrow \pi^*_{im}(200)$ (ILCT)	80	2.56	484	0.285	0.00	412
S_{11}	$n_{NCS}+d_{xz}(194) \rightarrow \pi^*_{im}(200)$ (LLCT)	77	2.74	452	0.087	0.00	-
	$n_{NCS}+d_{yz}(195) \rightarrow \pi^*_{im}(200)$ (LLCT)	10					
S_{12}	$\pi_{im}(193) \rightarrow \pi^*_{im}(200)$ (ILCT)	89	2.99	415	0.087	0.00	-

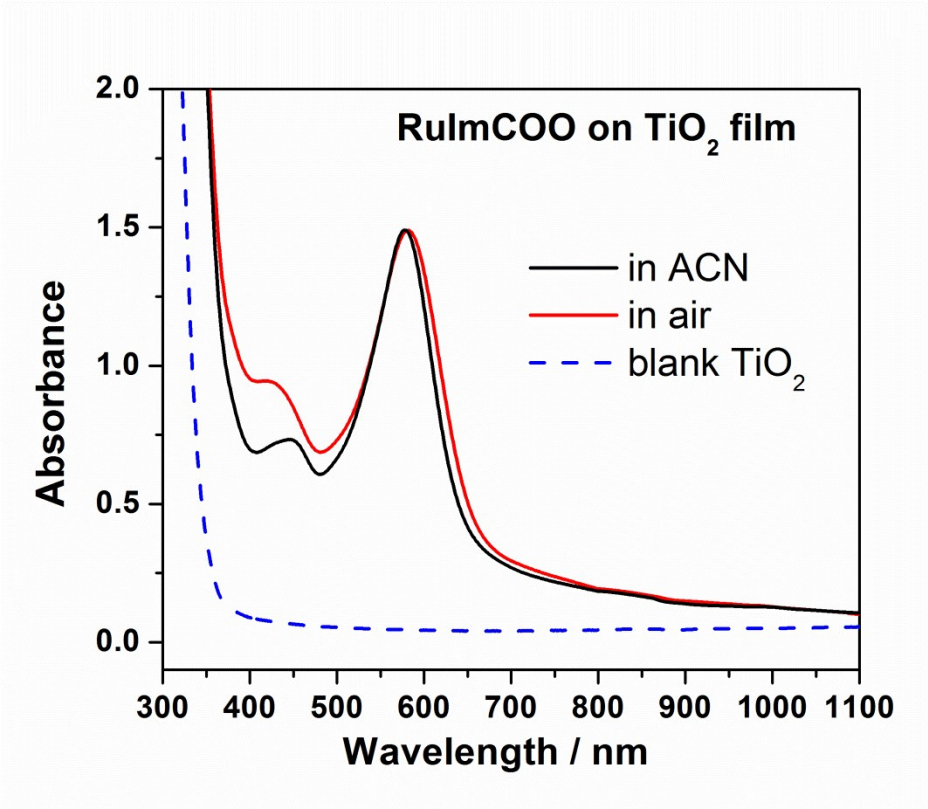

Figure S6. Absorption spectra of **RuImCOO** on TiO_2 film in ACN (black) and under air conditions (red) as well as a blank TiO_2 film (dash blue). The TiO_2 film shows negligible absorbance in the visible region, makes it feasible for SEC measurements of absorbed molecules.

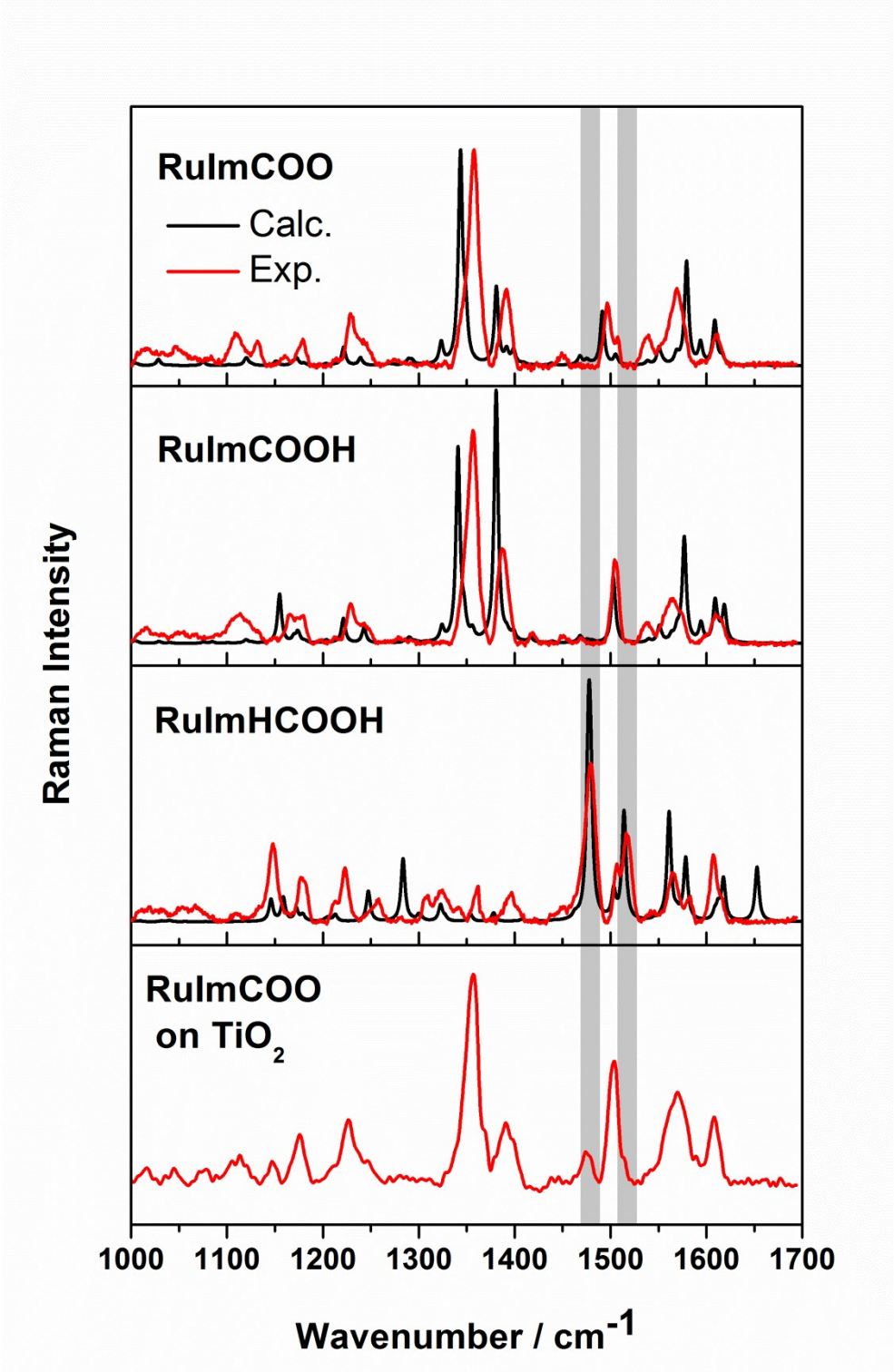

Figure S7. Calculated (black) and experimental (red) RR spectra of different protonation forms of **RuImCOOH** in ACN, as well as the RR spectra of **RuImCOO** on TiO_2, measured at 458 nm. Highlighted in grey are the locations of the signature bands of the protonated imidazole ring.

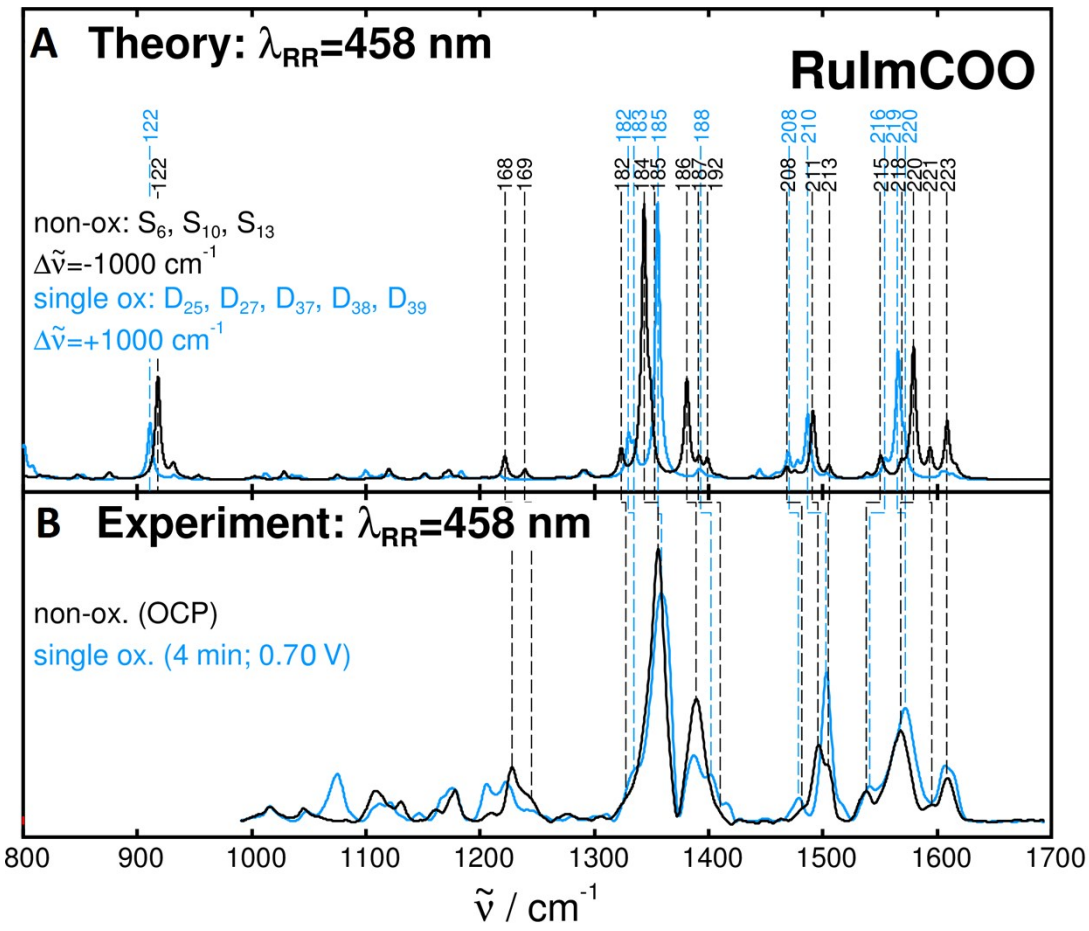

Figure S8. Calculated (A) and experimental (B) RR spectra of non-oxidized (blue) and oxidized (black) species of **RuImCOO** in solution (λ_{RR} = 458 nm), while the vibrational modes are assigned to the measured bands and labeled accordingly.

Table S9. Vibrational modes of the non-oxidized and oxidized species of **RuImCOO** with relative RR intensities ≥ 5% (λ_{RR} = 458 nm).

RuImCOO		
non-oxidized		
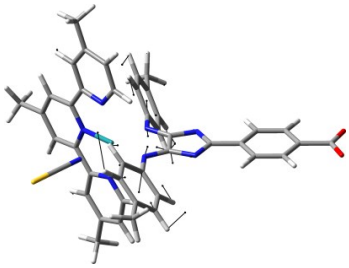	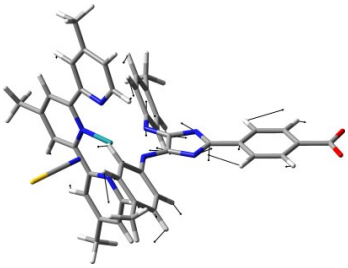	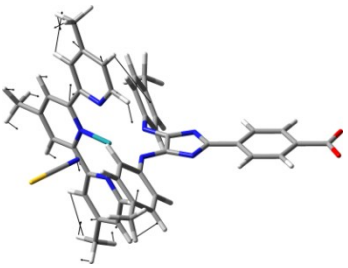
168	169	182
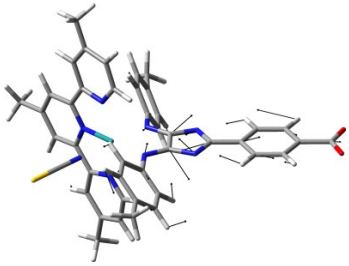	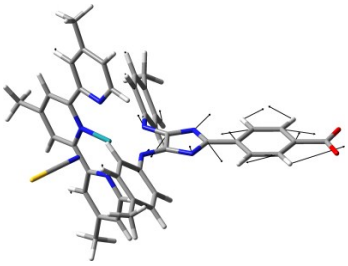	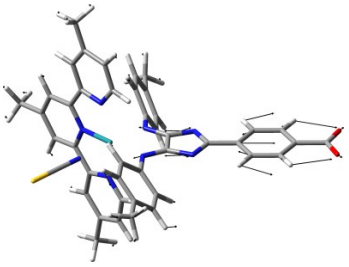
184	185	186
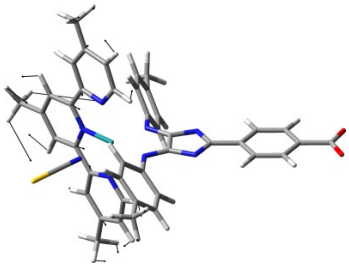	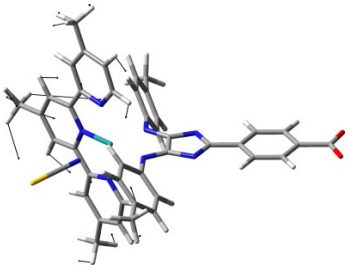	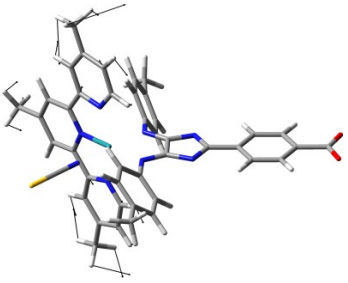
187	192	208
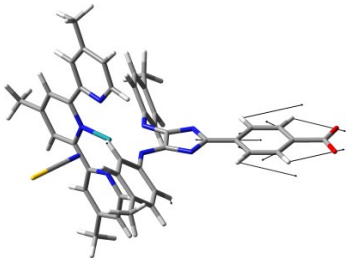	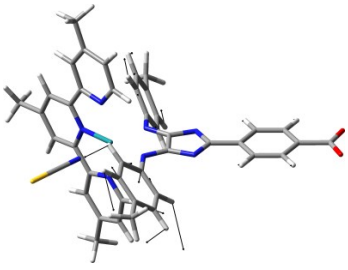	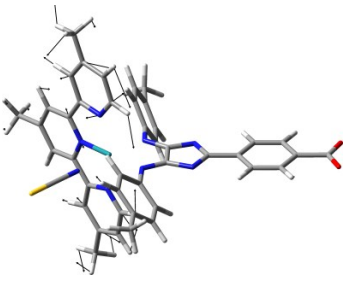
211	213	215

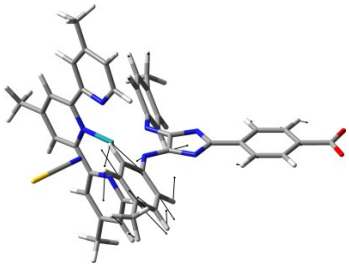 218	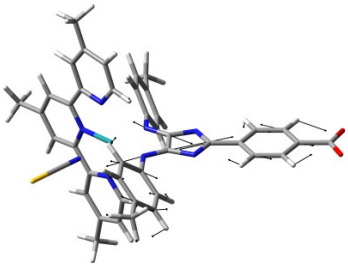 220	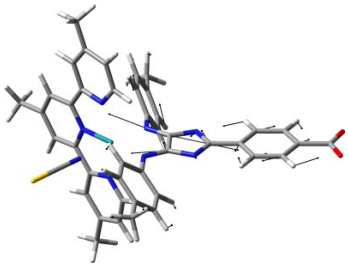 221
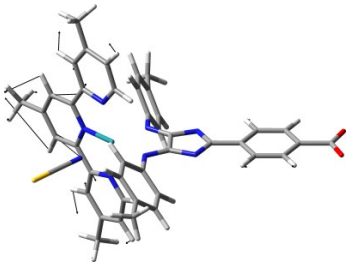 223		
single oxidized		
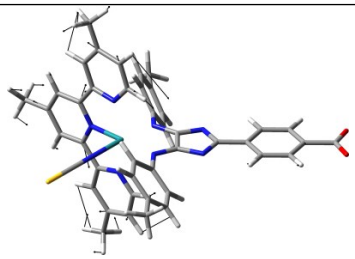 182	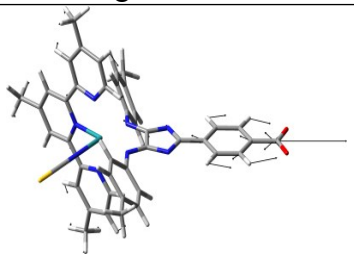 183	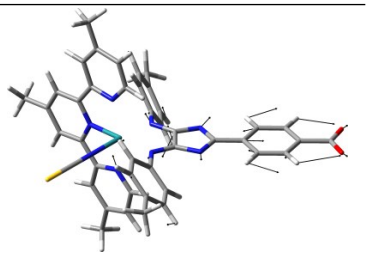 185
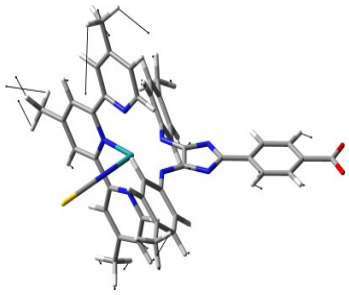 188	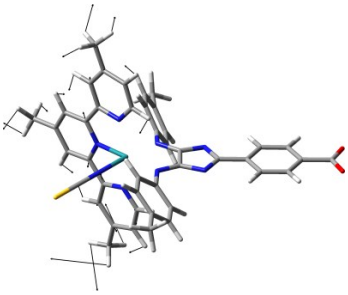 208	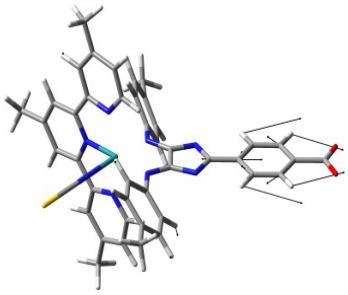 210
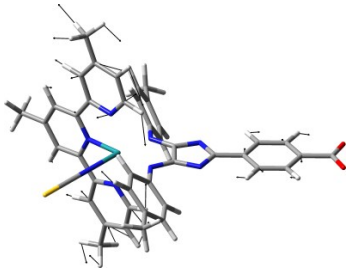 216	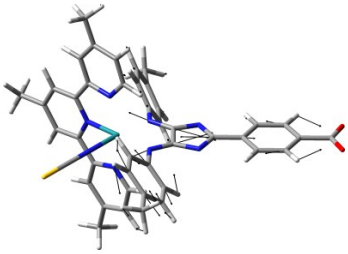 219	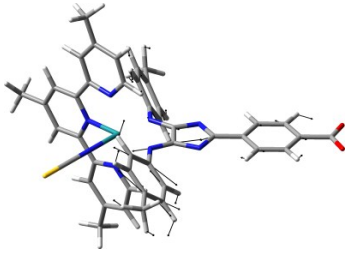 220